THE ASTROPHYSICAL JOURNAL, **219**:575–584, 1978 January 15

THE ROCKET-ULTRAVIOLET SPECTRUM AND MODELS OF THE PLANETARY NEBULA NGC 7662

RALPH C. BOHLIN
Goddard Space Flight Center
J. PATRICK HARRINGTON
University of Maryland
AND
THEODORE P. STECHER
Goddard Space Flight Center
Received 1977 May 16; accepted 1977 July 14

ABSTRACT

An ultraviolet spectrum of NGC 7662 was obtained with a rocket-borne telescope in a 130 s exposure by using a microchannel plate detector and film. The observed fluxes are given for both the lines and the continuum on an absolute basis. The correction for interstellar extinction with $E(B - V) = 0.22$ has been determined on the basis of the observed and calculated line ratios for the hydrogenic recombination line of He II at 1640 Å to Hβ. A detailed set of models of the thermal and ionization structure of NGC 7662 have been constructed for the purpose of interpreting the rocket observations. Predictions of three models are presented and compared with the ultraviolet as well as the existing visible, infrared, and radio observations. The spectral energy distribution of the central star for the models was specified so that the observed emission lines could be fitted. The resulting flux distribution is within 50% of a 100,000 K blackbody with some features which resemble recent spherical, non-LTE models but with a smaller discontinuity at 228 Å. The observed C III] intercombination line at 1909 Å and the C IV line at 1549 Å are best fitted with a solar carbon abundance and C/O ratio equal to unity. In order to obtain this fit, dielectronic recombination and charge exchange between neutral hydrogen and C IV were included, both of which increased the concentration of C III. The observed continuum consists of light from the central star and from the nebula, which contributes primarily via the two-photon process in H^0 and the Balmer continuum.

Subject headings: nebulae: abundances — nebulae: planetary — spectrophotometry — ultraviolet: spectra

I. INTRODUCTION

The planetary nebula is a state of evolution that a star near one solar mass passes through on its way to becoming a white dwarf. Quantitative models based on observations of the central star and the nebula predict the thermal and ionization structure and the emission-line intensities for any assumed chemical composition. Thus, by iterating on the initial assumption, we may derive the actual chemical composition. Modeling of planetary nebulae has been hindered by the fact that the strong carbon lines in the dominant stage of ionization lie in the rocket-ultraviolet. These C IV 1549 Å and C III] 1909 Å lines are important in controlling the thermal structure of the nebula through radiation; therefore they must be observed if satisfactory models are to be constructed. In addition, these lines accurately determine the carbon abundance for the first time. Since carbon is an early product of nucleosynthesis, any enhancement of carbon may indicate a mixing between the core and outer envelope, with considerable importance to theories of convection and stellar structure.

The observation of NGC 7662 seemed feasible following the successful observation of NGC 7027 in the rocket-ultraviolet by Bohlin, Marionni, and Stecher (1975) and a further test of the pointing and detection technology on the Orion Nebula (Bohlin and Stecher 1975). The bright planetary nebula NGC 7662 shows spectra of highly ionized species and is much less reddened than NGC 7027. Ultraviolet observations of NGC 7662 are particularly desirable, because the geometry seems to be spherical, making that planetary one of the best for theoretical study. However, the requirements on the STRAP IV pointing system were severe, since the target has to be within a few arcmin of the center of the 17′ by 24′ field of view. The pointing error of the STRAP IV is proportional to the distance from the first- or second-magnitude guide star used to update the gyros before moving to the target and holding on the rate-integrating gyros without active guidance. The successful observation of NGC 7662 at 16° from the guide star α And means that faint objects in the entire sky are now accessible to measurements with our instrument.

In addition to the three strong ultraviolet lines of

C III], C IV, and He II seen in NGC 7027, a new strong line of [Ne IV] at 2440 Å and a prominent continuum were measured in NGC 7662. The observations and the calibration are presented in the next two sections and the model calculations in § IV. The observed line strengths in the entire spectrum are compared with theory in § V. Finally, § VI contains ultraviolet continuum measurements and the predictions of the model.

II. OBSERVATIONS

The same payload that obtained the ultraviolet spectrum of NGC 7027 was flown on Aerobee 13.073 at 08ʰ00ᵐ UT on 1975 July 10 from the White Sands Missile Range. The microchannel plate (MCP) detector with the cesium telluride cathode was replaced, and a new emulsion batch of 35 mm Kodak IIa-O film recorded the spectra. As in the case of NGC 7027, two of the four surfaces were overcoated with the proper thickness of MgF_2 to minimize the sensitivity to Lα airglow. The laboratory dispersion of 46.41 Å mm^{-1} is linear to ± 1 Å from 1300 to 2800 Å. However, the flight exposures have a scale of 47.1 Å mm^{-1} determined by a fit to the four strong emission lines. This scale is accurate to ± 3 Å. The total absolute error in the initial pointing direction was under 1′. During the 130 s exposure on NGC 7662, the gyro drift was 20″ perpendicular to the dispersion and 20″ in the dispersion direction, producing emission lines with a full width at half-maximum (FWHM) of 20 Å. The limit cycle of $\pm 6''$ also contributed, somewhat, to degrading the instrumental resolution of 7″ and 7 Å.

III. ABSOLUTE CALIBRATION

All of the flight film and calibration frames were scanned with a 75 μm square aperture on a PDS densitometer. The accuracy of the calibration depends on the stability and reproducibility of that measuring device during the 10 minutes needed to measure a full 35 mm frame with a 560 by 480 point raster scan. The magnetic tape output is from an analog to digital converter with a 10 bit accuracy. Full scale of 1024 corresponds to a density of about 3. Repeated PDS measurements of the same area of film vary by as much as 5 parts in 1024, which generally produces an error of only 2% to 10% in the final fluxes, even for the low-contrast IIa-O film with a dynamic range of a factor of ~ 100. The uncertainty of ± 5 parts requires that each scan include a clear area of film to measure the zero shift. This zero-level adjustment, along with any variation in the clear film itself, dominates the error at low signal levels.

The relation between relative exposure level H and density D on the film was derived by using a constant light source and exposures between 2 and 256 s, assuming no reciprocity failure. This lack of reciprocity failure was confirmed to ± 10% by comparing the derived responses H for a range of exposure times and exposure levels differing by an order of magnitude on frames from flight and from the laboratory. No reciprocity failure is expected, because all light incident on the film has been amplified by the MCP with an electron gain of 600 to give an overall photon gain of 1100 at 2537 Å. The history of the MCP gain shows a monotonic increase, with a 60% rise in one year.

The absolute calibration relevant to NGC 7662 at the center of the field of view is based primarily on in-flight observations of the stars α Lyr and α And. Since these stellar spectra appear on the flight film strip along with the NGC 7662 spectrum, any uncertainties in developing the film or in the flight environment are automatically compensated. From the OAO-2 catalog of Code and Meade (1976) with the minor adjustments described by Bohlin, Strongylis, and Beeckmans (1976), the absolute flux of the calibration stars is known to ± 5% longward of 1700 Å and to ± 15% from 1300 to 1700 Å. The rocket did not obtain the predicted apogee and the observation of α Lyr was at the end of the flight. As a result, the spectrum was attenuated by O_2 shortward of 1800 Å. From 1800 to 2800 Å the calibrations from the two stars differ by a maximum of 12%, confirming the H and D curve and the accuracy of the densitometry. Independent laboratory calibrations, using the technique of Bohlin, Frimout, and Lillie (1974), as in previous rocket flights, and an additional calibration using a standard quartz-iodide lamp and a white Lambert surface, confirmed the in-flight absolute calibration to ± 30%. By combining the errors of approximately 10% each for the PDS, the H and D curve, the absolute fluxes of the stars, and the scatter in the two prime calibrations, we obtained an overall estimate of ± 20% for the accuracy of the final calibration.

The photographic spectrum of NGC 7662 is reproduced in Figure 1 (Plate 23), and the derived fluxes appear in Figure 2. The width of film used for the signal is as wide as the densest line at 1909 Å. The background noise level was determined from the part of the flight film adjacent to the NGC 7662 spectrum. The other spectrum above the planetary nebula is SAO 53026, a 7.6 mag F8 star. The grating dispersion plane for this stellar spectrum is separated by 3′ from that of NGC 7662, as expected from the planned roll orientation. The random pattern of small specks is the noise induced by charged particles, which is somewhat greater than observed in the laboratory.

The quantum statistics of the recorded signal can be estimated from the measured flux in the continuum of NGC 7662, the approximate quantum efficiency of 0.006 for the optics and the detector together, and the clear aperture of 520 cm^2 for the primary mirror. These statistics are consistent with the observed point-to-point scatter of $\sigma = \pm 10$% for the independent 75 μm (3.5 Å) sample intervals. Occasionally, a spike, like the one at 2125 Å, appears because of a small-scale cathode nonuniformity. In Table 1, each flux value is for a 50 Å bandpass and represents the average of 14 independent samples. The *statistical* uncertainty in the 50 Å mean fluxes is less than 4% in every case. The statistical uncertainty in the emission-line fluxes given in Table 2 is even less. However, the two shortest wavelength emission lines could be as

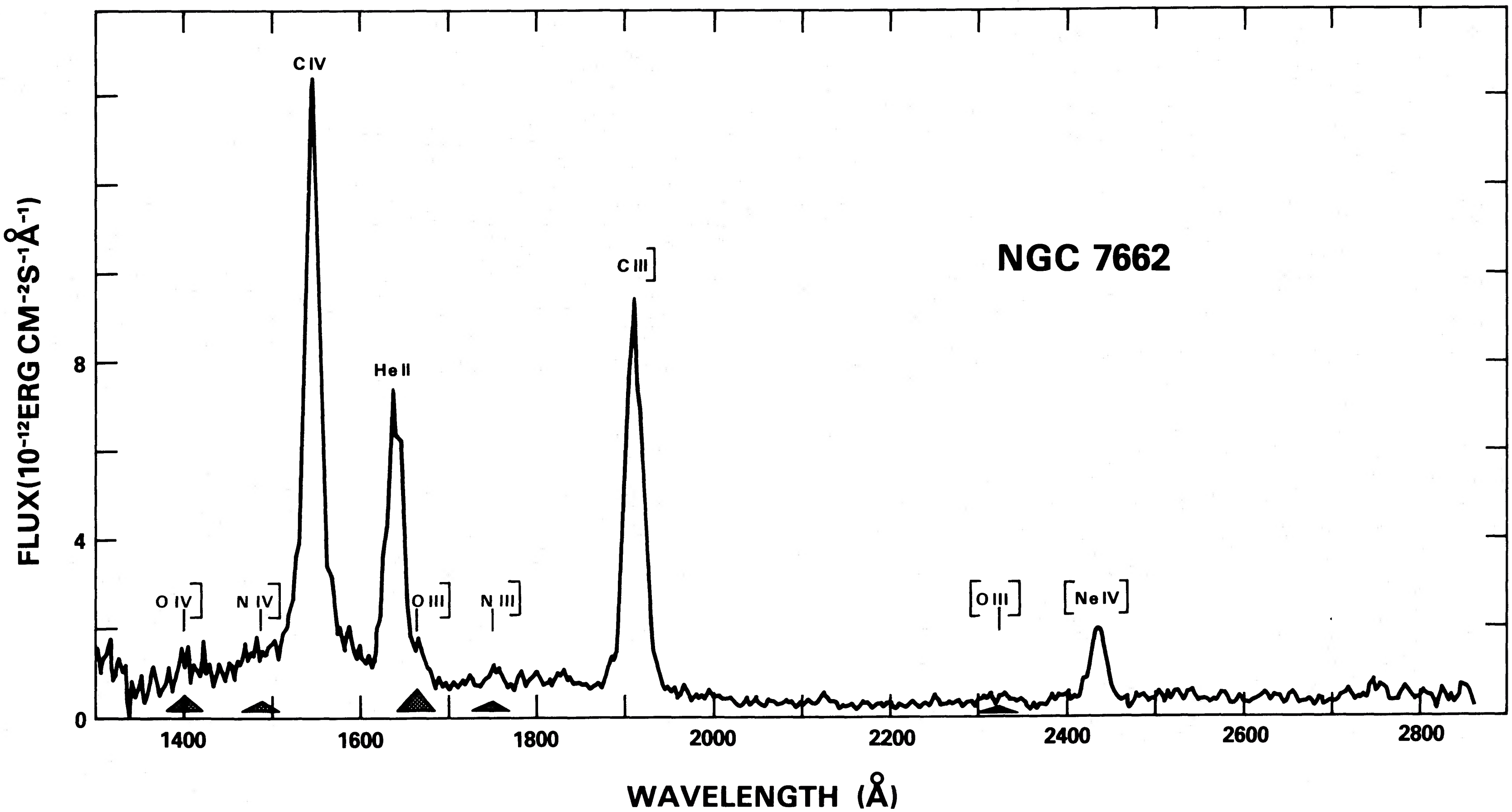

FIG. 2.—Absolute flux in the continuum of NGC 7662. The flux of the emission lines is equal to their area. Some weaker emission lines that are probably present are indicated by triangles, with areas predicted by the model and widths equal to the instrumental resolution.

TABLE 1

ULTRAVIOLET CONTINUUM FLUXES OF THE CENTRAL STAR PLUS NEBULA

λ (Å)	Obs. Flux (10^{-13} erg cm^{-2} s^{-1} Å^{-1})	Corr. Flux (10^{-12} erg cm^{-2} s^{-1} Å^{-1})	λ	Obs. Flux	Corr. Flux
1350	7.7	4.7	2150	3.1	2.4
1400	10.9	6.3	2200	2.8	2.1
1450	11.4	6.3	2250	3.1	2.1
1500	16	8.6	2300	3.8	2.2
1550	18	9.6	2350	3.4	1.9
1600	14.5	7.5	2400	4.5	2.2
1650	11	5.5	2450	4.5	2.1
1700	8.3	4.1	2500	4.6	2.0
1750	8.8	4.3	2550	4.4	1.9
1800	8.6	4.3	2600	3.9	1.6
1850	8.0	4.2	2650	4.0	1.6
1900	7	3.9	2700	4.0	1.5
1950	6	3.6	2750	5.4	1.9
2000	4.6	2.9	2800	4.7	1.6
2050	3.3	2.3	2850	4.5	1.5
2100	3.4	2.6			

TABLE 2

ULTRAVIOLET LINE FLUXES

λ (Å)	Ion	Obs. Flux (erg cm^{-2} s^{-1})	Corr. Flux (erg cm^{-2} s^{-1})
1549	CIV	2.77×10^{-10}	1.47×10^{-9}
1640	HeII	1.22	0.62
1909	CIII]	2.05	1.15
2440	[NeIV]	0.32×10^{-10}	0.15×10^{-9}

much as 15% stronger, if the continuum level was a plausible 25% lower from 1500 to 1675 Å. Owing to a rapid drop in signal level below 1500 Å, uncertainties in the background correction and in the toe of the *H* and *D* curve dominate and could be as large as ±50% at 1350 Å. Combining an additional 10% uncertainty for the continuum data, which are still near the toe of the *H* and *D* curve, with the 20% error bar on the absolute calibration produces a total error estimate of ±25% longward of 1675 Å.

Confirmation of the quoted error bars and of the *H* and *D* curve comes from a 32 s exposure that preceded the prime 130 s exposure. Despite the increase by a factor of 2 in the statistical error and more severe problems with the toe of the *H* and *D* curve, the fluxes derived from the 32 s exposure are usually within 20% and always within 40% of those in Table 1. A 6 s exposure on NGC 7662 was superior to the previous spectrum of NGC 7027 obtained in 90 s.

IV. THE MODELS

Several detailed models of the thermal and ionization structure of NGC 7662 have been constructed for the purpose of interpreting the ultraviolet spectrum. Although models of this nebula have been published by Flower (1969), Harrington (1969), and Kirkpatrick (1972), comparison with the observations of Peimbert and Torres-Peimbert (1971) suggests that the problem should be reexamined. One obvious defect of the earlier models is the high helium abundance. Any change in this parameter implies large changes in the ionization structure of a high-excitation nebula.

Our models include the ions of H, He, C, N, O, Ne, and S. The photoionization cross sections are from Flower (1968), Henry (1970), and Chapman and Henry (1971). The values of the collision cross sections used are in Osterbrock (1974), except for C^+ and N^{2+} from Jackson (1972); O^+ and S^+ from Pradhan (1976); and N^+, O^{2+}, and Ne^{2+} from Seaton (1975). The radiative recombination rates of Tarter (1971, 1973) were used. The $O^0 + H^+ \rightleftarrows O^+ + H^0$ charge exchange process was included by using the rates of Field and Steigman (1971). Since dielectronic recombination can be important for C^{2+} (Bohlin, Marionni, and Stecher 1975), this process was included for all ions using the rates of Aldrovandi and Péquignot (1973). Another physical process which has a significant effect on the C^{2+} ionic abundance is the $C^{3+} + H^0 \rightarrow C^{2+} + H^+$ charge exchange reaction. The rate is from Blint, Watson, and Christensen (1976).

After an initial model is constructed using the on-the-spot approximation, the diffuse radiation is evaluated at each point in the nebula by integration of the transfer equation. The sources of the diffuse field include recombination to the ground states of H^0, He^0, and He^+, recombinations to the $n = 2$ level of He^+, two photon decays from He^+ $2s$ and He^0 2^1S, single photon decays from He^0 2^3S, and some of the line radiation produced by the Bowen fluorescence mechanism. Following the analysis of Harrington (1972), 30% of the He^+ Lα photons are converted to $2p^2\ ^3P_1$–$2p3d\ ^3P_2{}^o$ O III line photons which escape the line due to Doppler shifts, while 50% lead to population of the $2s^22p3s$ term which decays with the production of O III lines that are able to ionize the gas. We assume that the conversion of the He^+ Lα photons to the escaping O III line radiation occurs at the point of He^{2+} recombination and neglect any further scattering of these end products of the Bowen mechanism. The nebular models are iterated 3 times to obtain an ionization structure which is consistent with the diffuse radiation field it generates.

Photographs of NGC 7662 show that it has a double shell structure (Aller 1956; Weedman 1968). The nebula is modeled by two concentric spherical shells, each with a Gaussian density distribution in the radial coordinate. For the adopted distance of 1 kpc to the nebula, the radii of the density maxima of the shells are 0.031 and 0.065 pc. The thicknesses of the shell at half-maximum density are 0.0054 and 0.00113 pc, respectively.

To construct a model, one must specify the flux of ionizing stellar radiation. Monochromatic photographs of this nebula in the light of He II $\lambda4686$ show that He^{2+} is confined to the inner shell (Aller 1956), implying that the nebula completely absorbs stellar radiation with $\lambda < 228$ Å. Thus, a He II Zanstra temperature for the central star can be deduced from the strength of He II $\lambda4686$ and the ultraviolet continuum measurements as discussed in § VI. Assuming a blackbody flux distribution, this temperature is 100,000 K. As is well known, the H I Zanstra temperature of this nebula is much less than the He II temperature, which means that for a blackbody energy

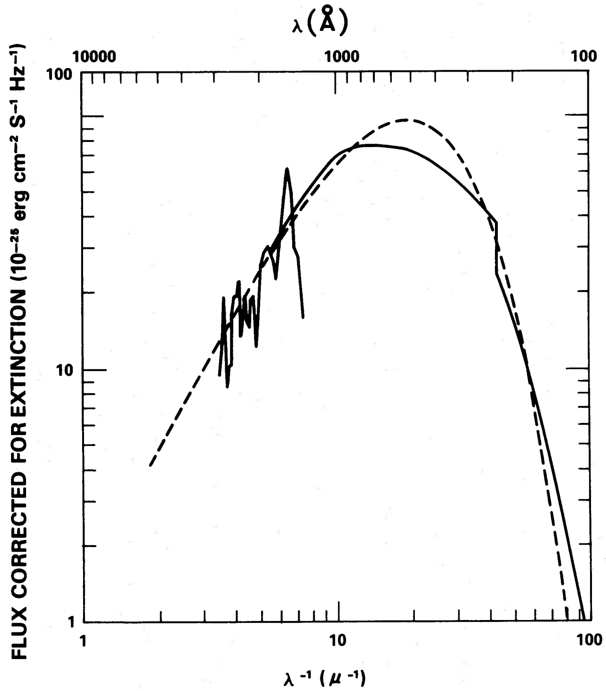

FIG. 3.—*Smooth solid line*, flux of the central star of NGC 7662 used in the model calculations. *Jagged solid line*, the ultraviolet continuum minus the calculated nebular emission. *Dashed line*, a 100,000 K blackbody normalized to the observations at 1800 Å.

distribution the nebula must be optically thin at the H^0 Lyman limit (see Harman and Seaton 1966). Consequently, the amount of the low-ionization species such as O^+ and N^+ is too small and the model line intensities for [O II] and [N II] are much weaker than observed. Model-atmosphere flux distributions (e.g., Hummer and Mihalas 1970; Kunasz, Hummer, and Mihalas 1975) only make matters worse, because they have a large drop in flux at 228 Å. Any model chosen with the required flux for $\lambda < 228$ Å will have an excess of radiation for $\lambda > 228$ Å.

The adopted flux distribution is shown in Figure 3 and has been modified from a 100,000 K blackbody distribution in the following manner: (1) A modest drop has been introduced at 228 Å, since all model-atmosphere calculations show some drop at this wavelength. (2) The flux distribution for $\lambda < 228$ Å is flatter than the blackbody curve while preserving the number of photons, in order to produce the necessary fraction of Ne^{4+} ions. (3) The flux between 912 and 228 Å is flatter than the blackbody and depressed with respect to it. Most model-atmosphere calculations, especially those with extended structure, have a distribution which is flattened with respect to a blackbody curve. Depressing the flux helps with the problem of the lower-ionization stages mentioned above. The stellar flux is treated as a free parameter, but this seems reasonable considering the uncertain state of the model-atmosphere calculations (e.g., no models include line-blanketing effects). The stellar luminosity corresponding to the adopted flux is $2.55 \times 10^3 L_\odot$.

In order to obtain the proper amount of the lower-ionization species, even with our adopted flux distribution, the outer shell must be optically thick at the Lyman edge. To simultaneously obtain the proper Hβ flux, the outer shell is fragmented in the models. Only 13% of this shell is actually filled with material; the radiation passes freely through the other 87%. Photographs do show a lumpy structure in the outer shell (Aller 1956). In our final models, the maximum density in the smooth inner shell is 9.3×10^3 H atoms and ions cm^{-3}, while the maximum in the fragments of the outer shell is 6.7×10^3.

V. THE EMISSION LINES

a) *Extinction and the Visual Lines*

For comparison of the models with the observed visual spectrum of NGC 7662, the photoelectric scanner observations of Peimbert and Torres-Peimbert (1971, hereafter PTP) are used for those lines which they have observed. For the [O II] and [S II] lines they employed a 30″ diaphragm, and a 21″ diaphragm for the other lines. Unfortunately, even 30″ will not include all of the outer ring of NGC 7662. Since the [N II] radiation is concentrated in the outer ring, the observations of Osterbrock, Capriotti, and Bautz (1963) are used for the [N II] $\lambda\lambda$6548, 6584/Hα ratios along with PTP's Hα/Hβ ratio. The adopted [O III] λ4363 is based on the [O III] λ5007/λ4363 ratio of Bohuski, Dufour, and Osterbrock (1974) normalized to the PTP value for λ5007; this differs only slightly from the PTP value for λ4363. The individual components of the [O II] $\lambda\lambda$3726, 3729 and the [S II] $\lambda\lambda$4069, 4076 doublets are obtained from the intensities of PTP and the ratios quoted by Aller and Epps (1976). Other line intensities are from Aller, Kaler, and Bowen (1966), which refer to the bright ring of the nebula, and from O'Dell (1963), who remarks that in most cases "the object was larger than the entrance slit." These observations, corrected for reddening by using $E(B-V) = 0.224$ and the reddening curve of Code *et al.* (1976), are expressed relative to Hβ = 100 in Table 3. The color excess of $E(B-V) = 0.224$ is derived from the ratio of the measured absolute fluxes of the He II λ1640 to Hβ, in comparison with the predicted ratio from the best-fitting model. The observed flux of λ1640 is corrected for the predicted flux of O III] λ1666 located in the wing of the He II Hα line. As for the case of NGC 7027, the mean extinction curve from Code *et al.* (1976) is adopted for all extinction calculations. Pottasch *et al.* (1977*a*) obtain $E(B-V) = 0.30$ from the depth of the 2200 Å extinction dip in ANS photometry. Since they did not subtract the line emission in their 2500 and 3300 Å bands, 0.30 is an overestimate of the extinction (see § VI).

The observed visual line intensities were used to constrain the parameters defining our models as follows: (1) The densities and filling factor discussed above were chosen to produce the observed Hβ flux at the adopted distance of 1 kpc. The absolute Hβ flux of 9.75×10^{-11} ergs $\text{cm}^{-2}\,\text{s}^{-1}$ from PTP is corrected to the Hayes and Latham (1975) scale. A subtraction of 3.75% was made to account for the Brackett δ line of He II. The reddening of $E(B-V) = 0.224$ and the extinction curve of Code *et al.* (1976) imply a corrected Hβ flux of 2.05×10^{-10} ergs $\text{cm}^{-2}\,\text{s}^{-1}$. (2) The adopted stellar flux determines the He ionization balance producing a He II λ4686 intensity that matched the observations. (3) The abundance of helium is chosen so that the He I λ5876 line intensity is close to the observed value. (4) The temperature within the nebula is sensitive to both the carbon and the oxygen abundance. For a given C/O ratio, the abundance relative to hydrogen is adjusted to obtain the observed temperature, as determined by [O III] λ5007/λ4363 ratio. (5) By raising the density and lowering the filling factor of the outer shell to the values given above, the strengths of the [O II] $\lambda\lambda$3726, 3729 lines were brought up to the observed values. Since the effects of the N, Ne, and S abundances on the structures of the nebula are secondary, they can be adjusted independently to fit the observed line intensities of the respective elements.

b) *Comparison of the Lines and the Models*

Table 3 contains the line intensities of three models with C/O ratios of 1.0, 1.35, and 0.5. The best fit overall is provided by C/O = 1. The visual lines match the observed spectrum better than any previously published model. The only intensities which are not well reproduced are those of [S II], in particular, the $\lambda\lambda$6716, 6731 doublet. The sulfur abundance was chosen to fit the [S III] and [S IV] lines, since most of the sulfur is present as S^{2+} and S^{3+} (20% and 44%, respectively); only 2.7% is S^{+}. The [S II] radiation is very strongly concentrated toward the outer edge of the model and is very sensitive to the optical depth of the outer shell. We also note that the observed intensity of [S II] $\lambda\lambda$6716, 6731 given by Noskovia (1976) is 4 times higher than the PTP value quoted in Table 3. The 5 GHz flux agrees to within the uncertainties of the collected observations graphed by Terzian (1968), confirming our corrections for interstellar absorption.

The predicted intensity of the [Ne IV] $\lambda\lambda$2439, 2441 ultraviolet doublet is close to the observed value. The neon abundance was determined by the [Ne III] lines, and the ionization structure of neon in the models is further constrained by the [Ne V] lines. Thus, the good fit of the [Ne IV] lines, which arise in the inner shell and are sensitive to the temperature there, confirms the model of the hot He^{2+} zone.

The predicted intensity of the ultraviolet doublet of C III] is about 25% weaker and that of C IV about 25% stronger than the rocket observations. Varying the C/O ratio in the model only improves one doublet at the expense of the other. Furthermore, models with C/O = 0.5 or 1.35 produce [O III] lines which are too strong or too weak, respectively. There are two physical processes which influence the C^{2+}/C^{3+}

TABLE 3

OBSERVATIONAL FLUXES AND THE PREDICTIONS OF THREE MODELS

λ (Å)	Ion	Corr. † Flux	Ref.	Model Fluxes C/H = 3.7×10^{-4} O/H = 3.7×10^{-4}		C/H = 4.45×10^{-4} O/H = 3.3×10^{-4}		C/H = 2.2×10^{-4} O/H = 4.4×10^{-4}	
997	CIII	–	–	16.7		18.2		14.1	
991	NIII	–	–	0.39		0.36		0.50	
1032, 38	OVI	–	–	0.17		0.13		0.31	
1214, 18	OV]	–	–	4.6		3.6		8.2	
1239	NV	–	–	4.9		4.4		6.8	
1243	NV	–	–	2.5		2.2		3.5	
1402	OIV]	*	–	21		16.6		33	
1487	NIV]	*	–	10.7		9.9		13.5	
1548	CIV	720	BHS	590	890	660	1000	430	650
1551	CIV			300		330		220	
1575	[NeV]	–	–	0.13		0.12		0.18	
1640	HeII	300	BHS	300		300		300	
1666	OIII]	*	–	27		24		34	
1750	NIII]	*	–	8.3		8.2		9.0	
1815	[NeIII]	–	–	0.33		0.33		0.35	
1907	CIII]	560	BHS	270	430	320	500	181	290
1909	CIII]			158		185		107	
2321	[OIII]	*	–	4.1		3.7		5.0	
2439	[NeIV]	74	BHS	30	63	29	60	36	74
2441	[NeIV]			33		31		39	
2470	[OII]	–	–	1.19		1.08		1.39	
3203	HeII	–	–	11.3		11.3		11.3	
3343	[NeIII]	0.46	AKB	0.23		0.23		0.24	
3346	[NeV]	5.4	AKB	4.8		4.5		5.6	
3426	[NeV]	12.3	AKB	12.7		12.0		14.9	
3722	[SIII]	0.66	AKB	0.71		0.72		0.73	
3726, 29	[OII]	14.6	PTP	13.7		12.3		16.0	
3869	[NeIII]	76	O	75		76		75	
3968	[NeIII]	23	AKB	22		22		22	
4069	[SII]	0.60	PTP	0.97	1.29	0.95	1.27	0.98	1.31
4076	[SII]			0.32		0.32		0.33	
4363	[OIII]	15.9	BDO, PTP	15.3		13.7		18.5	
4471	HeI	2.7	PTP	2.6		2.6		2.6	
4686	HeII	44	PTP	43		43		43	
4715	[NeIV]	2.0	AKB	0.31	0.82	0.28	0.75	0.39	1.04
4725	[NeIV]			0.51		0.47		0.65	
4861	Hβ	100	–	100		100		100	
4959	[OIII]	400	O	390		350		460	
5007	[OIII]	1150	PTP	1140		1030		1350	
5412	HeII	5.4	O	3.5		3.5		3.5	
5755	[NII]	0.17	AW	0.14		0.14		0.14	
5876	HeI	6.8	PTP	7.1		7.1		7.0	
6300	[OI]	–	–	0.14		0.12		0.17	
6312	[SIII]	–	–	1.25		1.26		1.28	
6548	[NII]	2.6	OCB	1.87		1.86		1.89	
6563	Hα	310	M	287		287		287	
6584	[NII]	5.6	OCB	5.4		5.4		5.5	
6716, 31	[SII]	0.93	PTP	5.7		5.5		5.8	
7318	[OII]	1.18	PTP	0.20	1.48	0.19	1.35	0.24	1.73
7319	[OII]			0.62		0.56		0.72	
7330	[OII]			0.34		0.30		0.39	
7331	[OII]			0.33		0.30		0.38	
9069	[SIII]	9.0	O	10.5		10.5		10.6	
9532	[SIII]	29	N	25		26		26	
105200	[SIV]	44	GMS	37		37		37	
128100	[NeII]	–	–	1.13		1.12		1.14	
187100	[SIII]	–	–	7.5		7.5		7.7	
5GHz	Radio	0.7f.u.	T	0.76f.u.		0.76f.u.		0.75f.u.	
λ5007/λ4363	[OIII]	72	BDO	75		75		73	
λ3729/λ3726	[OII]	0.56	AE	0.58		0.58		0.58	
λ6716/λ6731	[SII]	0.66	AE	0.67		0.67		0.67	

*These lines are marked by triangles in Figure 2. † F(Hβ) = 100 = 2.05×10^{-10} erg $cm^{-2} s^{-1}$, corrected for E(B-V) = 0.224.

References for Table 3

AE	Aller and Epps (1976)	M	Miller (1973)
AKB	Aller, Kaler, and Bowen (1966)	O	O'Dell (1963)
AW	Aller and Walker (1970)	OCB	Osterbrock, Capriotti, and Bautz (1963)
BDO	Bohuski, Dufour, and Osterbrock (1974)	PTP	Peimbert and Torres - Peimbert (1971)
BHS	Bohlin, Harrington, and Stecher - this paper	T	Terzian (1968)
GMS	Gillet, Merrill and Stein (1972)	N	Noskovia (1976)

ionization ratio in the model, in addition to photoionization and radiative recombination. First, C^{2+} is the only ion in our models with an important contribution from dielectronic recombination. Second, the $H^0 + C^{3+} \rightarrow H^+ + C^{2+}$ charge exchange process is also significant, despite the relatively low number of H^0 atoms, because the rate is so high. If charge exchange is neglected in the C/O = 1 model, the C III] intensity drops by 12% and the C IV intensity increases by 6%. (The model of NGC 7027 discussed by Bohlin, Marionni, and Stecher 1975 shows a 30% increase in the C III] intensities when charge exchange is included.) If *neither* charge exchange nor dielectronic recombination is included, the C III] intensity drops by 45% and the C IV lines strengthen by 23%. Since the rate coefficients of dielectronic recombination and, especially, the charge exchange process are uncertain, the C^{2+}/C^{3+} ratio in the model is consistent with the observations.

As in the case of NGC 7027 discussed by Bohlin, Marionni, and Stecher (1975), the C IV doublet is optically thick. In NGC 7662 the optical thickness of the inner shell at the center of the C IV λ1548 line is 2.0×10^3, somewhat less than in the model of NGC 7027 because of the thin shell geometry. Thus these line photons must be scattered many times before escaping. But unlike NGC 7027, NGC 7662 has almost no infrared excess (Cohen and Barlow 1974) and, presumably, very little dust. So unless there is some other mechanism for destruction of the C IV photons, the line should not be attenuated.

If the models do underestimate the C^{2+}/C^{3+} ratio for some reason (e.g., incorrect atomic rates), a change in this ratio would not have a very large effect on the temperature of the nebula. While the collision cross section of the C IV doublet is larger than that of the C III] doublet, the C III] lines have a lower excitation potential. As a result, C^{3+} is only about 20% more efficient in cooling the gas than C^{2+} at the temperature of the inner shell (~14,000 K). Thus, a change in the C^{2+}/C^{3+} ratio would change primarily the relative intensities of the C III] and C IV lines and have only a secondary effect on the total energy radiated by carbon. The observed sum of intensities of C III] + C IV is 1280, while the models with C/O = 1, 1.35, and 0.5 predict 1320, 1500, and 940, respectively. Therefore, the determination of C/H = 3.7×10^{-4} is more accurate than the fit to either the C III] or C IV lines alone.

TABLE 4

ELEMENTAL ABUNDANCES RELATIVE TO HYDROGEN

	NGC 7662*	NGC 7662†	Sun‡
He	0.92	0.094	...
C	3.7×10^{-4}	6.3×10^{-3}	3.7×10^{-4}
N	8.0×10^{-5}	4.3×10^{-5}	1.15×10^{-4}
O	3.7×10^{-4}	4.5×10^{-4}	6.8×10^{-4}
Ne	7.0×10^{-5}	...	1.1×10^{-4}
S	8.0×10^{-6}	...	1.6×10^{-5}

* This paper.

† Torres-Peimbert and Peimbert 1977.

‡ Withbroe 1971, with Ne/O ratio from Bertsch *et al.* 1972.

c) *Elemental Abundances*

Table 4 summarizes the abundances derived from our models and from other measurements. NGC 7662 is one of the 44 planetary nebulae studied by Torres-Peimbert and Peimbert (1977, hereafter TPP). Since we have adopted most of their observed line intensities, the results should be directly comparable. The helium abundances are in agreement. Their value for oxygen is slightly higher, probably because they assume temperature fluctuations more extreme than those in our models. Our nitrogen abundance is higher than TPP for three reasons. First, their value is based upon the assumption that $N^+/N = O^+/O$, which overestimates N^+/N by 36%, according to our model. Second, TPP assume a temperature of 9400 K for the [O II] and [N II] emitting regions, which is about 2000 K lower than in our models. In addition, we have adopted a value for the observed [N II] λ6584 line intensity which is 40% higher than the TPP value.

Hawley and Miller (1977) obtained a sulfur abundance of 4.5×10^{-6} from the analysis of [S II] lines at six different positions in NGC 6720. They express concern that this value is much less than solar. For NGC 7662, however, our abundance of 8.0×10^{-6} yields a ratio of S/O = 0.022, which is in good agreement with the solar ratio of 0.024.

The carbon abundances that TPP derive for NGC 7662 and 18 other nebulae are based upon the faint recombination lines of C II and C III. The values they obtain are very high, clearly in disagreement with our results from the UV carbon lines. Such high carbon abundances would cool a nebula drastically. We have constructed a model with the TPP abundances and find that the temperature in the nebula drops by 4000 K in the inner shell and by 2000 K in the outer shell, with the result that the UV carbon lines are too strong and the visual [O III] lines too weak. Therefore, the carbon recombination lines do not give reliable abundances.

The solar abundances are systematically higher than our results for NGC 7662. Planetary nebulae cover a range of population types, and this object seems to have a deficiency of heavy elements. However, the carbon abundance is about solar, and thus carbon is enhanced relative to other heavy elements. Since planetary nebulae are thought to be ejected from stars which have undergone both CNO cycle hydrogen burning and helium shell burning, and since the products of these reactions could be mixed into the envelope prior to its ejection, the relative abundances of C, N, and O in planetaries may be important to theories of nucleosynthesis. The C/O ratio of unity found here may support the suggestion by Zuckerman *et al.* (1976) that some, if not most, planetary nebulae evolve from carbon stars (defined by a C/O ratio greater than unity). They propose an evolutionary sequence of the form: carbon star → infrared source such as CRL 2888 → planetary nebula. This hypothesis has not been tested, because the carbon abundance in planetary nebulae has been unknown.

VI. THE CONTINUUM

At the 20″ resolution of the ultraviolet data, the stellar spectrum is convolved with the nebular continuum. Therefore only the sum predicted for the flux from the star and nebula can be compared with the measurements. The total nebular flux for the C/O = 1 model is shown in Figure 4 for the major continuum emission processes, including the Balmer, Paschen, and Brackett recombination of hydrogen; the two-photon emission of hydrogen; the He^{2+} Paschen and Brackett spectra; and the free-free emission from electrons colliding with H^+, He^+, and He^{2+}. The discontinuity at 2050 Å is due to He^{2+} Brackett recombination. At the shorter wavelengths, the nebular continuum is mostly due to two-photon emission, as was found by Gurzadyan (1976).

At 1800 Å, the nebular flux can be subtracted from the total continuum to give an accurate value for the stellar flux, since the star is almost twice as bright as the nebula. The flux at 1800 Å and the total number of photons at $\lambda < 228$ Å from the He II λ4686 line imply a Zanstra, equivalent blackbody temperature of 100,000 K. This blackbody curve is illustrated in Figure 3 and the Rayleigh-Jeans tail is shown in Figure 4. Since the long-wavelength flux distribution is not expected to be strongly dependent on the details of the atmospheric structure, the actual stellar magnitude should be close to the predicted value of V = 13.0, which includes 0.7 mag of reddening. However, the best measurement is probably V = 11.8 (Shao and Liller, unpublished), a factor of 3 brighter.

A factor of 3 error in the ultraviolet fluxes is considerably outside the measurement errors. Independent flux values from the ANS (Pottasch 1975, personal communication) confirm the rocket measurements and strengthen this conclusion. The broad-band ANS values denoted by A in Figure 4 include the entire nebula in the 2.′5 field of view. The 2500 Å ANS point has been corrected by 28% for the presence of the [Ne IV] 2440 Å line in the 150 Å bandpass; and at 3300 Å, 37% of the ANS signal is due to the λ3343 and λ3346 lines of [Ne III] and [Ne V] listed in Table 3, together with the Bowen fluorescent lines of O III at 3299, 3312, and 3341 Å (see Pottasch *et al.* 1977*b*).

In summary, the ultraviolet continuum of NGC 7662 can be represented by the sum of a blackbody

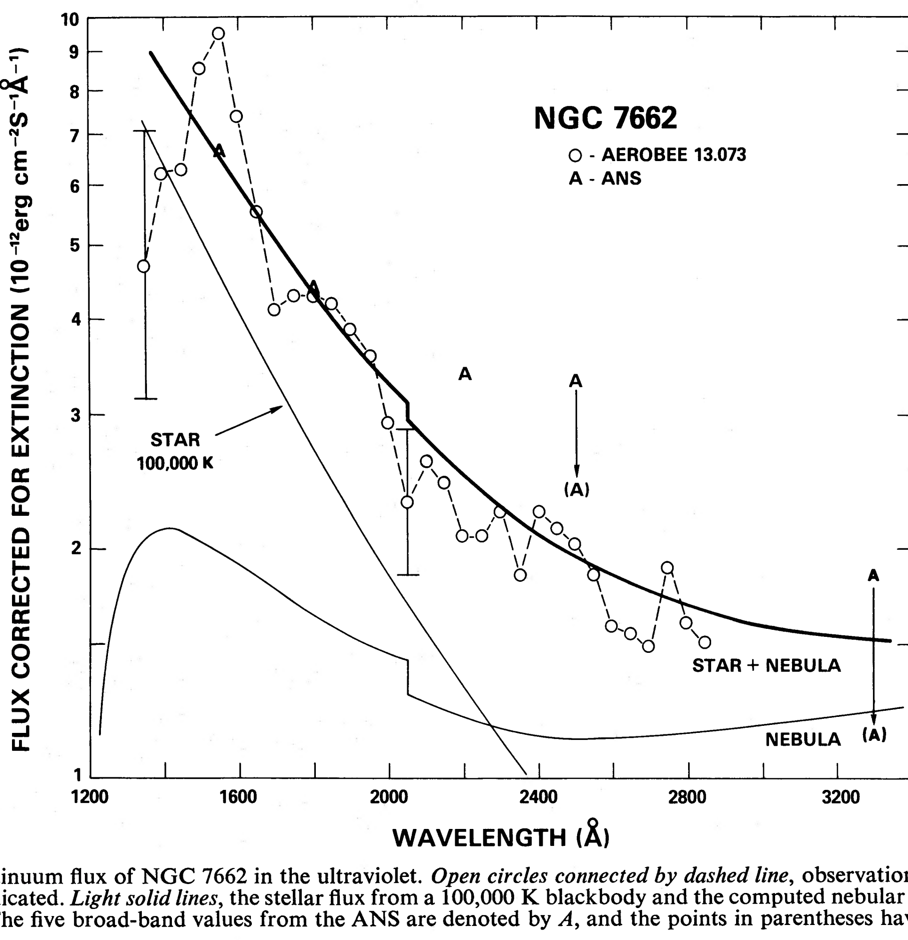

FIG. 4.—Continuum flux of NGC 7662 in the ultraviolet. *Open circles connected by dashed line*, observations from Table 1 with typical errors indicated. *Light solid lines*, the stellar flux from a 100,000 K blackbody and the computed nebular flux; *heavy solid line*, star + nebula. The five broad-band values from the ANS are denoted by A, and the points in parentheses have been corrected for emission lines.

continuum at 100,000 K and the computed nebular continuous emission. The precision of the agreement is generally within 25%, consistent with the error bars expected for the measurements of both the rocket spectrum and the ANS photometry.

The launch support crew for Aerobee 13.073, including G. Baker and T. Collinson, produced another flawless performance for the entire system. In particular, A. K. Stober assembled the optics and mechanics of the payload, operated the laboratory and payload vacuum systems, and handled all the photographic processing, including the preparation of Figure 1. The densitometry was done on the area-scanning PDS densitometer at the U.S. Department of Agriculture with the aid of P. Hopkins. R. D'Angelo helped with the calibration and data reduction. P. A. Marionni suggested that the O III] line at λ1666 might make a contribution to the He II feature at 1640 Å. J. P. H. acknowledges support by a Faculty Research Award from the University of Maryland General Research Board. Computer time for the construction of models was provided by the Computer Science Center of the University of Maryland.

Note added in manuscript.—After this paper was submitted for publication, Christensen, Watson, and Blint (1977) made available the charge-exchange cross section for N IV–H. A model was calculated including the $N^{+3} + H \rightarrow N^{+2} + H^{+}$ reaction, with the result (in agreement with the sense of our observations) that the N IV concentration was reduced and the N III concentration increased. Since the N III concentration in part determines the N II line intensities which we used to establish the nitrogen abundance, our result for nitrogen in Table 4 must be reduced by 60%. Furthermore, Dalgarno (1977) has pointed out that N III, as well as a number of other ions, should have a large cross section for charge exchange, implying an even larger reduction in the abundance of nitrogen. Until good charge-exchange cross sections are available for all the relevant ions, abundances will remain somewhat uncertain.

We also wish to clarify the calculated ratio of C III] λ1907/λ1909 which is sensitive to the collision strengths between the fine-structure levels of the $2s2p^3P^0$ state. The ratio of 1.7 presented in Table 3 was obtained using the collision strengths of Blaha (1968), which did not include the effect. The collision strengths given by Eissner (1972) yield a ratio of 1.27 for our model, in agreement with Loulergue and Nussbaumer (1976). The total strength of the doublet changes by less than 1%.

REFERENCES

Aldrovandi, S. M. V., and Péquignot, D. 1973, *Astr. Ap.*, **25**, 137.
Aller, L. H. 1956, *Gaseous Nebulae* (London: Chapman & Hall).
Aller, L. H., and Epps, H. W. 1976, *Ap. J.*, **204**, 445.
Aller, L. H., Kaler, J. B., and Bowen, I. S. 1966, *Ap. J.*, **144**, 291.
Aller, L. H., and Walker, M. F. 1970, *Ap. J.*, **161**, 917.
Bertsch, D. L., Fichtel, C. E., and Reames, D. V. 1972, *Ap. J.*, **171**, 169.
Blaha, M. 1968, *Ann. d. Ap.*, **31**, 311.
Blint, R. J., Watson, W. D., and Christensen, R. B. 1976, *Ap. J.*, **205**, 634.
Bohlin, R. C., Frimout, D., and Lillie, C. F. 1974, *Astr. Ap.*, **30**, 127.
Bohlin, R. C., Marionni, P. A., and Stecher, T. P. 1975, *Ap. J.*, **202**, 415.
Bohlin, R. C., and Stecher, T. P. 1975, *Bull. AAS*, **7**, 547.
Bohlin, R. C., Strongylis, G. J., and Beeckmans, F. 1976, Proc. 16th General Assembly of the IAU in Grenoble.
Bohuski, T., Dufour, R. J., and Osterbrock, D. E. 1974, *Ap. J.*, **188**, 529.
Chapman, R. D., and Henry, R. J. W. 1971, *Ap. J.*, **168**, 169.
Christensen, R. B., Watson, W. D., and Blint, R. J. 1977, *Ap. J.*, **213**, 712.
Code, A. D., Davis, J., Bless, R. C., and Hanbury Brown, R. 1976, *Ap. J.*, **203**, 417.
Code, A. D., and Meade, M. 1976, University of Wisconsin preprint.
Cohen, M., and Barlow, M. J. 1974, *Ap. J.*, **193**, 401.
Dalgarno, A. 1977, *IAU Symposium No. 76, Planetary Nebulae*, in press.
Eissner, W. 1972, in *The Physics of Electronic and Atomic Collisions*, ed. T. R. Grovers and F. J. de Heer (Amsterdam: North-Holland), p. 460.
Field, G. B., and Steigman, G. 1971, *Ap. J.*, **166**, 59.
Flower, D. R. 1968, in *IAU Symposium No. 34, Planetary Nebulae*, ed. D. E. Osterbrock and C. R. O'Dell (Dordrecht: Reidel), p. 205.
———. 1969, *M.N.R.A.S.*, **146**, 243.
Gillett, F. C., Merrill, K. M., and Stein, W. A. 1972, *Ap. J.*, **172**, 367.
Gurzadyan, G. A. 1976, *Pub. A.S.P.*, **88**, 891.
Harman, R. J., and Seaton, M. J. 1966, *M.N.R.A.S.*, **132**, 15.
Harrington, J. P. 1969, *Ap. J.*, **156**, 903.
———. 1972, *Ap. J.*, **176**, 127.
Hawley, S. A., and Miller, J. S. 1977, *Ap. J.*, **212**, 94.
Hayes, D. S., and Latham, D. W. 1975, *Ap. J.*, **197**, 593.
Henry, R. J. W. 1970, *Ap. J.*, **161**, 1153.
Hummer, D. G., and Mihalas, D. 1970, *M.N.R.A.S.*, **147**, 339.
Jackson, A. G. R. 1973, *M.N.R.A.S.*, **165**, 53.
Kirkpatrick, R. C. 1972, *Ap. J.*, **176**, 381.
Kunasz, P. B., Hummer, D. G., and Mihalas, D. 1975, *Ap. J.*, **202**, 92.
Loulergue, M., and Nussbaumer, H. 1976, *Astr. Ap.*, **51**, 163.
Miller, J. S. 1973, *Mém. Soc. Roy. Sci. Liège*, Ser. 6, **5**, 57.
Noskovia, R. I. 1976, *Astr. Zhurnal*, **53**, 1210.
O'Dell, C. R. 1963, *Ap. J.*, **138**, 1018.
Osterbrock, D. E. 1974, *Astrophysics of Gaseous Nebulae* (San Francisco: Freeman).
Osterbrock, D. E., Capriotti, E. R., and Bautz, L. P. 1963, *Ap. J.*, **138**, 62.
Peimbert, M., and Torres-Peimbert, S. 1971, *Bol. Obs. Tonantzintla y Tacubaya*, **6**, 21 (PTP).
Pottasch, S. R., Wesselius, P. R., Wu, C.-C., and van Duinen, R. J. 1977*a*, *Astr. Ap.*, **54**, 435.
Pottasch, R. R., Wu, C.-C., Wesselius, P. R., and van Duinen, R. J. 1977*b*, preprint.
Pradhan, A. K. 1976, *M.N.R.A.S.*, **177**, 31.
Seaton, M. J. 1975, *M.N.R.A.S.*, **170**, 475.
Tarter, C. B. 1971, *Ap. J.*, **168**, 313.
———. 1973, *Ap. J.*, **181**, 607.
Terzian, Y. 1968, in *IAU Symposium No. 34, Planetary Nebulae*, ed. D. E. Osterbrock and C. R. O'Dell (Dordrecht: Reidel), p. 87.
Torres-Peimbert, S., and Peimbert, M. 1977, *Rev. Mexicana Astr. Astrofisica*, submitted (TPP).
Weedman, D. W. 1968, *Ap. J.*, **153**, 49.
Withbroe, G. L. 1971, in *The Menzel Symposium*, ed. K. B. Gebbie (NBS Special Pub. 353), p. 127.
Zuckerman, B., Gilra, D. P., Turner, B. E., Morris, M., and Palmer, P. 1976, *Ap. J.* (*Letters*), **205**, L15.

RALPH C. BOHLIN and THEODORE P. STECHER: Laboratory for Astronomy and Solar Physics, Code 680 Goddard Space Flight Center, Greenbelt, MD 20771

J. PATRICK HARRINGTON: Astronomy Program, University of Maryland, College Park, MD 20742

1978ApJ...219..575B

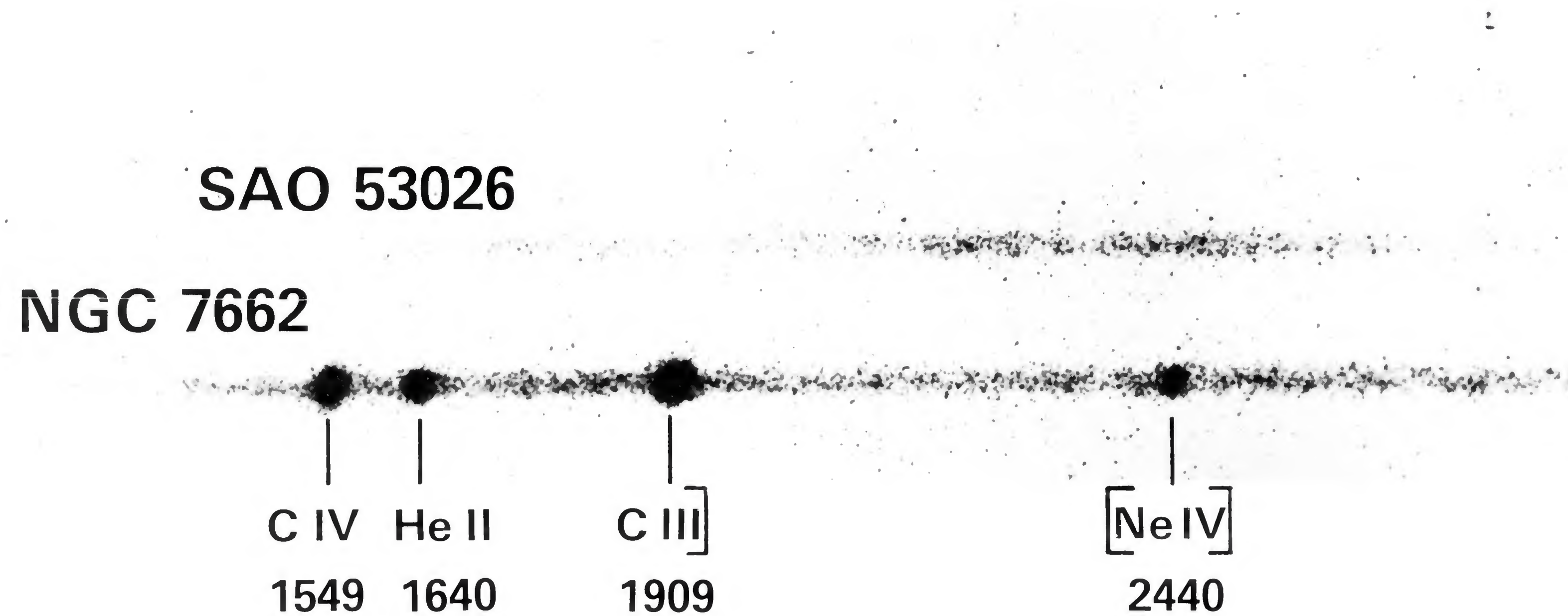

FIG. 1.—Photographic spectrum of the planetary nebula NGC 7662. The strong ultraviolet emission lines are labeled. Also included in the narrow field of the objective spectrograph is SAO 53026, a 7.6 mag F8 star. Exposure time was 130 s.

BOHLIN *et al.* (*see* page 576)